AIAA Guidance, Navigation, and Control Conference and Exhibit
5-8 August 2002, Monterey, California

AIAA 2002-4656

Method of Slewing the Spacecraft to Minimize Settling Time*

Hong-Jen Chen† and Brij N. Agrawal‡

Spacecraft Research and Design Center
Naval Postgraduate School, Monterey, California 93943

The low-frequency flexible modes of solar arrays on spacecraft are excited by the minimum-time bang-bang control during a slew maneuver. These flexible modes limit the control bandwidth and degrade the pointing error at the end of slew maneuver, resulting in a longer settling time. The objective of this investigation is to develop and verify methods to shape the torque profile of reaction wheels for the slew maneuver such that, at the end of slew, vibration are minimized and the settling time is reduced. Effectiveness of the smooth versine input profiles, torque feedforward, and input shaping are accessed. Both numerical simulation results and ground simulated experimental results are presented in this paper.

1. Introduction

In many spacecraft maneuvers, slewing with the shortest time is very desirable. However the bang-bang control, which is the minimum-time optimal control solution to the problem, excites the low-frequency modes of flexible appendages such as solar arrays on spacecraft. As a result, the flexible modes limit the control bandwidth and degrade the pointing error at the end of slew maneuver, resulting in a longer settling time. So researchers over the years developed several shaping techniques to smooth the minimum-time solutions [1-5].

Development and implementation of improved techniques to minimize attitude errors at the end slew of a flexible spacecraft, decreasing the settling time, has been an active area of research at the Naval Postgraduate School for the last ten years. A Flexible Spacecraft Simulator (FSS) was developed in the early 90s to validate experimentally the effectiveness of designed control laws. In the beginning our emphasis was to evaluate smooth torque profile for the momentum wheel to minimize the vibrations at the end of slew [6, 7]. Next the emphasis shifted to developing closed loop switching function for on-off thruster firing to minimize vibration at the end of slew [8], then on shaping torque command to ensure zero residual vibration of flexible [9].

In this paper, we develop and verify methods to shape the torque profile of momentum wheels for the slew maneuver such that, at the end of slew, the vibration are minimized and the settling time is reduced. Effectiveness of the smooth versine input profiles, torque feedforward, and input shaping [10] are accessed. Both numerical simulation results and ground simulated experimental results are presented in this paper.

2. The flexible spacecraft simulator (FSS)

The flexible spacecraft simulator (FSS) simulates motion about the pitch axis of a spacecraft. As shown in Figure 1, it is comprised of a rigid central body, which represents the main body of the spacecraft, and a flexible appendage, which represents a flexible antenna support structure. The flexible appendage is composed of a base beam cantilevered to the main body and a tip beam rigidly connected to the base beam at a right angle. Five air pads on a granite table support the FSS and its flexible appendage to minimize the friction during motion.

The simulator has a reaction wheel and two cold gas thrusters installed for actuation as actuators. In this investigation, however, we use only the reaction wheel. Measurement of the motion is accomplished by an RVDT (Rotation Variable Displacement

* This work was performed while the first author held a National Research Council Research Associateship Award at Spacecraft Research and Design Center, Naval Postgraduate School, Monterey, CA
† Ph.D., US National Research Council Associate Fellow
‡ Professor and Director, AIAA Associate Fellow

Transducer) as the position sensor and a rate gyro as the velocity sensor. The data acquisition and control function of the experiments is performed by the combination of a dSPACE DS1103 controller board and a host personal computer. The real-time code is developed on the host machine using graphical models in MATLAB/SIMULINK from the Mathworks Inc., and in C for certain task-specific blocks in the models. The models are compiled within the SIMULINK environment with integrated function provided by dSPACE, and downloaded to the control board for implementation.

3. Simulation model of FSS

In this section a brief introduction to the simulation model of the flexible spacecraft simulator (FSS) is given to each of its building blocks, including the dynamics modelling of the flexible appendage and the main body, the calculation of natural frequencies, the formulation of system equations for control simulation, the feedback control system, and the design of torque profiles are introduced.

3.1. Flexible Dynamic Model of the Flexible Spacecraft Simulator

The flexible dynamic model of FSS used in this study was derived [6] using the hybrid-coordinate formulation [11]. The flexible appendage was modeled using the finite element method. The equations describing the motion of the FSS are

$$I_{zz}\ddot{\theta} + \sum_{i=1}^{n} D_i \ddot{q}_i = T_c + T_d \tag{3.1}$$

$$\ddot{q}_i + 2\zeta_i \omega_i \dot{q}_i + \omega_i^2 q_i + D_i \ddot{\theta} = 0, \quad i = 1 \ldots n \tag{3.2}$$

where θ is angular position of the main body, q_i is modal coordinate for the ith cantilever mode, I_{zz} is the moment of inertia of the whole system, D_i is rigid-elastic coupling for the ith mode, T_c is the control torque, T_d is the disturbance torque, ζ_i is the damping ratio of the ith mode, and ω_i is the natural frequency for the ith mode.

The rigid elastic coupling D_i is given by

$$D_i = \int_F \left(x_F \phi_i^y - y_F \phi_i^x \right) dm \tag{3.3}$$

where x_F and y_F are coordinates of a point on the flexible structure, and ϕ_i^x and ϕ_i^y are the x and y component of ith modal vector at that point, respectively.

3.2. System Natural Frequencies of the FSS

To find the natural frequencies of the FSS, the equations are formulated as a second order partitioned system with the damping ratios set as zero:

$$\begin{bmatrix} I_{zz} & D^T \\ D & I \end{bmatrix} \begin{Bmatrix} \ddot{\theta} \\ \ddot{q} \end{Bmatrix} + \begin{bmatrix} 0 & 0 \\ 0 & \lambda \end{bmatrix} \begin{Bmatrix} \theta \\ q \end{Bmatrix} = \begin{Bmatrix} T_C + T_D \\ 0 \end{Bmatrix} \tag{3.5}$$

where

$$\lambda = \begin{bmatrix} \ddots & & \\ & \omega_i^2 & \\ & & \ddots \end{bmatrix} \text{ and } D = \begin{Bmatrix} D_1 \\ D_2 \\ \vdots \\ D_n \end{Bmatrix}$$

After normalization and similarity transformation, the system natural frequencies are found by solving the associated eigenvalue problem. A MATALB built-in routine is used to obtain the numerical values as listed in Table 1.

3.3. State Space Formulation for FSS System Control

For the simulation of the control of the flexible spacecraft simulator, the second order dynamics model in section 3.1 is formulated in the state space form. The state space representation of the system is

$$\begin{cases} \dot{x} = Ax + Bu \\ y = Cx + Du \end{cases} \tag{3.4}$$

where

$$x = \begin{bmatrix} \theta & q_1 \cdots q_n & \dot{\theta} & \dot{q}_1 \cdots \dot{q}_n \end{bmatrix}^T,$$

$$y = \begin{bmatrix} \theta & \dot{\theta} \end{bmatrix}^T,$$

$$A = \frac{1}{I_{zz}^0} \begin{bmatrix} 0 & 0 & \cdots & 0 & I_{zz}^0 & 0 & \cdots & 0 \\ 0 & 0 & \cdots & 0 & 0 & I_{zz}^0 & \cdots & 0 \\ \vdots & \vdots & \ddots & \vdots & \vdots & \vdots & \ddots & \vdots \\ 0 & 0 & \cdots & 0 & 0 & 0 & \cdots & I_{zz}^0 \\ 0 & F_1 & \cdots & F_n & 0 & H_1 & \cdots & H_n \\ 0 & -G_1 & \cdots & -D_1 \cdot F_n & 0 & -J_1 & \cdots & -D_1 \cdot H_n \\ \vdots & \vdots & \ddots & \vdots & \vdots & \vdots & \ddots & \vdots \\ 0 & -D_n \cdot F_1 & \cdots & -G_n & 0 & -D_1 \cdot H_1 & \cdots & -J_n \end{bmatrix}^T$$

$$B = \frac{1}{I_{zz}^0} \begin{bmatrix} 0 & 0 & \cdots & 0 & 1 & -D_1 & \cdots & -D_n \end{bmatrix}^T,$$

$$C = \begin{bmatrix} 1 & 0 & \cdots & 0 & 0 & 0 & \cdots & 0 \\ 0 & 0 & \cdots & 0 & 1 & 0 & \cdots & 0 \end{bmatrix},$$

$$D = \begin{bmatrix} 0 & 0 \end{bmatrix}^T,$$

with

$$I_{zz}{}^0 = I_{zz} - \sum_{i=1}^{n} (D_i)^2$$

$$F_i = D_i \omega_i^2,$$

$$G_i = \omega_i^2 I_{zz}^0 + D_i F_i,$$

$$H_i = 2\xi_i \omega_i D_i, \text{ and}$$

$$J_i = 2\xi_i \omega_i I_{zz}^0 + D_i H_i$$

3.4. Feedback Control System

As shown in Figure 2, the feedback control system for simulation is simply a PID controller with optional torque feedforward. The angular and velocity response of the main body (θ and $\dot{\theta}$) are directly connected as the position and rate feedback, except the signals are both passed through a low pass 5th order Butterworth filter with a cut-off frequency at 3 Hz. No additional measurement dynamics are modelled.

3.5. Design of the Torque Profiles

The input torque profiles of the FSS are designed based on the following assumptions: (1) the inertia of the main body is dominantly larger of those of the flexible appendage and the reaction wheel, (2) the flexible appendage moves with the main body as a rigid body, i.e., the cross-coupling effect from the flexible modes are neglected, (3) the loss of control torque due to the friction in the reaction wheel is negligible, and (4) the disturbance torque, T_d, is negligible comparing to the control torque, T_c.

Three types of command profiles are investigated, including bang-bang, smoothed bang-bang, and versine Profiles. Due to the close performance of the later two, the results are demonstrated using only the bang-bang and the versine profiles. Figures 3 and 4 show the desired torque profiles in this investigation. Both profiles have a symmetrical acceleration period followed by a symmetric deceleration period. The amplitudes of the two periods are identical with opposite direction therefore a stop-to-stop maneuver is generated for the FSS. The analytical expressions for the bang-bang and the versine profiles are given as the following.

bang-bang Profile:

$$\begin{cases} 1, & 0 \le t \le t_1 \\ -1, & t_1 < t \le t_2 \\ 0, & t_2 < t \end{cases}$$

versine Profile:

$$\begin{cases} \frac{1}{2}\left[1 - \cos\left(\frac{\pi t}{t_A}\right)\right], & 0 \le t \le t_A \\ 1, & t_A \le t \le t_B \\ \frac{1}{2}\left[1 - \cos\left(\frac{\pi (t_1 - t)}{t_A}\right)\right], & t_B \le t \le t_1 \\ -\frac{1}{2}\left[1 - \cos\left(\frac{\pi (t - t_1)}{t_A}\right)\right], & t_1 < t \le t_C \\ -1, & t_C \le t \le t_D \\ -\frac{1}{2}\left[1 - \cos\left(\frac{\pi (t_2 - t)}{t_A}\right)\right], & t_D \le t \le t_2 \\ 0, & t_2 < t \end{cases}$$

The smooth parameter α for the versine profile, whose value is between 0 and 1, is defined as $\alpha = 2 * t_A / t_1$. Note that the versine Profile reduces to the bang-bang profile when α is set to zero.

Figures 5 and 6 show the input-shaped versions of the profiles in Figure 3 and 4, respectively. The input shaping referred here is the method developed by Singer and Seering [10]. The technique is based on linear system theory and specifies vibratory systems of any order as cascaded set of second-order poles with decaying sinusoidal response. It generate multiple impulses so that later impulses will cancel out the system vibration caused by the previous impulses, therefore produces a net positive motion with no vibration or the derivatives of vibration after the input has ended at the time of the last impulse.

In our implementation of the input shaping, two methods – Zero Vibration Derivative (ZVD) and Zero Vibration Derivative Derivative (ZVDD) – are used. In theory the ZVD method should produce no vibration and neither does its derivative. The ZVDD method, in addition should achieve even zero derivative of the derivative of the vibration. These methods are noted by many authors allow plant uncertainties on the order of 40% while retaining the zero-vibration characteristics.

As shown Figures 5 to 8, the slew time of the bang-bang profiles are lengthened by either smoothing using versine curves or input shaping. The versine smoothing lengthens the slew time by 2.365 seconds, and the input shaping with ZVD method further lengthens it by 5.133 seconds.

4. Simulation Results

The simulation of the slew maneuver of the flexible spacecraft simulator is performed in the

MATLAB/SIMULINK environment (version R12). The simulation period is 30 seconds to match the length of each experiment. The simulation solver is ode45 (Dormand-Prince) with a maximum fixed step size of 0.001 second matching the sample time of the whole model.

The physical parameters of the FSS are set as I_{zz}= 7.874 Kgm^2 (obtained from the experiments), D_i is calculated as [-0.9334, -0.6018, -0.0463, -0.0545, -0.0306, -0.0273, -0.0195, -0.0113], and the damping ratios are assumed as 0.01 for all modes. The cantilever and system frequencies are shown in Table 1. These frequencies are obtained from a 16-mode finite element model, but only 8 modes are included in the entire system for simulation of control response.

The slew angle is set to 10 degree with two tolerances for residual vibration chosen as 0.015 and 0.0015 degree. The control gains of the PID controller are Kp = 200 volts/deg, Ki = 10 volts/(deg*sec), and Kv = 100 volts/(deg/sec). The torque for designing the command profile is set as 70% of the true maximum to allow for the feedback torque variation. The simulation results are presented in Figures 7 to 15 and Tables 2 to 3. Observation and comparison of all these cases are detailed in the following sub-sections. Here the cases and their corresponding figures are first explained.

Figures 7 to 10 shows the residual vibration of FSS at the end of slew, with the simulator being controlled by various methods. Figure 7 corresponds to the baseline case of FSS being controlled by PID control (using proportional and rate feedback) with any torque feedforward or input shaping. Control method in Figure 8 is the same as Figure 7, except this time the torque feedforward is applied. For Figure 9, input shaping (of the first two modes using ZVD method) is applied instead, in addition to the baseline cases in Figure 7. Then both torque feedforward and input shaping of two modes using ZVD method, are applied in the cases in Figure 10. In Figure 11 an extra case of input shaping only the first mode using the ZVD method is also run and put together with the cases of shaping either zero or two modes to access the effect of shaping different number of modes.

Figures 12 to 15 demonstratesZVD runs presented in Figures 7 to 11, and their results regarding settling time and maximum residual vibration are summarized in Table 2 and 3. Figure 7 shows .

4.1. Effect of Torque Feedforward

In this section we investigate the effect of applying torque feedforward on reducing the maximum residual vibration after slew, i.e., we compare the results in Figure 8 to those in Figure 7, and the results in Figure 10 to those in Figures 9. The settling times of all these case are summarized in the upper part of Table 2. All of the cases show great improvement in performance no matter the input is smoothed by versine or not, and no matter the input is shaped or not.

As for maximum residual vibration, we look at the results summarized in Table 3 and compare the upper four cases (#1 ~ #4) to the lower four cases (#5 ~ #8). Again we see great reductions in all of the four cases sets – (#1, #5), (#2, #6), (#3, #7), and (#4, #8). In those rows bellow the rows showing the values of the maximum residual vibration, the improvement are characterized in terms of percentage with the comparing case specified in front. The improvement range is from 61.6% to 89.1%.

4.2. Effect of Input-Shaping of the Torque Profiles

In this section we investigate what improvement input-shaping the torque profiles will do for the residual vibration and settling. To see this we compare the left columns to the right columns in Tables 2 and 3. We found out that input shaping is very effective in reducing the residual vibration and settling time, no matter torque if feedforward or not, and no matter the input is smoothed by versine or not. The reduction of maximum vibration ranges between 88.1% and 98.2%.

4.3. Effect of Smoothing with versine Profiles

In this section we investigate whether smoothing the bang-bang type of profiles with versine curves is also effective in bringing down the residual vibration and shortening the settling time. After comparing columns two to columns one and columns four to columns three, in both Table 2 and Table 3, it is obvious that the smoothing is also effective in reducing residual vibration and settling time. The improvement ranges from 27.4% to 70.6% from each bang-bang type of input profile.

4.4. Effect of Input-shaping Multiple Flexible Modes

In this section we compare the results corresponding to Figure 11, with FSS being control by PID controller (with rate and position feedback) and torque feedforward also applied, the three input profiles are versine with input shaping of zero, one, or two modes with the ZVD method. The resultant maximum residual vibrations are 0.0257, 0.00127, and 0.001degree. Therefore shaping 1 mode is very effective; it brings down the maximum residual

vibration by 95.1%. Shaping an extra mode, the second mode, also helps. It further reduces by 21.1%.

4.5. Sensitivity to Errors in Natural Frequencies in Input Shaping

Figures 12 through 15 demonstrate the robustness of input shaping performance, in terms of residual vibrations and settling time, to the errors in the natural frequencies being shaped. Both shaping methods of ZVD (Figures 12 and 14) and ZVDD (Figures 13 and 15) are explored. The residual vibration of the non-shaped versine input with smoothing factor of 1 is 0.46764 degree. The percentage residual vibration (vibration with shaping divided by vibration without shaping) of the ZVD case for the entire Figure 12 is under 2.35%, and under 1% for the ZVDD in Figure 13. Both methods are quite robust to the frequency errors for this type, so is the case for the settling times in Figures 14 and 15.

4.6. Conclusion of Simulation Results

All of the techniques, smoothing bang-bang profile with versine curves, torque feeding forward, and input shaping with ZVD or ZVDD methods are all very effective in reducing the maximum residual vibrations and the settling time. When stringent pointing requirement are imposed, we should apply as many techniques of the three as possible.

5. Experimental Results

All parameter values used in experiment and in the simulation are set to be exactly the same. The inertias of the main body and the reaction wheel are identified as 7.874 and 0.1089 $Kg*m^2$ assuming the disturbance negligible. The control law applied in all experiments is PID control (using position and velocity feedback from RVDT and rate gyro sensors) with torque feedforward always applied. The control gains used in the experiments are [Kv, Ki, Kp] = [100V/(deg/s), 200V/deg, 10V/(deg*s)] as in the simulations. All input profiles in experiments are extended for 5 seconds at the beginning to allow the feedback control to bring back the simulator to its zero position. The results in experiment basically confirm the same conclusions in simulations.

5.1. Identification of system rotational inertias and flexible modes

The rotational inertias of reaction wheel and the simulator main body are first identified for the generation of the feedforward torque. Applying constant control torque for several seconds forces the reaction wheel and the main body to accelerate uniformly. Then the accelerations and the inertias are obtained from least squares fit. The frequencies of the first two flexible modes are identified from manual excitation of the simulation flexible appendage and the use of an accelerometer attached on the main body to identify the free-free mode frequencies. The first two free-free modes are identified as 0.2667 Hz and 0.75 Hz, which are very close those obtained from the finite element model.

5.2. Effect of Smoothness of the Torque Profiles

Figures 16 shows the results corresponding to bang-bang input and versine profile with smooth factor of 1. The maximum residual vibration decreased from 0.213 degree to 0.144 degree, which is a 32.3% reduction. Other smooth factor smaller than one are also run in experiment and confirmed that the larger the smooth factor, the smaller the residual vibration.

5.3. Effect of Input-Shaping of the Torque Profiles

Figures 17 and 18 show the improvement on vibration reduction with input shaping of the first one or two modes using the ZVD method, on bang-bang profile and versine profile with smoothing factor of 1.0 respectively. The results of maximum residual vibration and settling are summarized in Table 4 and Table 2 (bottom two rows). Same conclusion is drawn as from the simulations: shaping the first mode is very effective in reducing residual vibrations (by 83.9 and 73%), and shaping one more mode – the second mode – introduces further reduction (11.3% and 2.9%).

5.4. Sensitivity to Errors in Natural Frequencies in Input Shaping

Figure 19 demonstrates the performance robustness of input shaping to the errors in the natural frequencies, in terms of residual vibrations, using either ZVD or ZVDD method. The ZVDD method appears more insensitive to frequency errors.

6. CONCLUSIONS

In the investigation, both the simulation and experimental results showed the effectiveness of the

application of torque feedforward, input shaping, and smoother profiles. It is found out that when tight tolerance on the attitude performance is required, input shaping is effective in achieving a desirable settling time which cannot be easily achieved when using only versine smoothing and torque feedforward. Furthermore the performance of the input shaping is robust within big range of frequency error. With as much as 20% error in natural frequencies input shaping still improves performance. Note that input shaping is very desirable when the pointing tolerance is stringent, but the use of it is not recommended when the original desired slew time is very short and there are significant low frequency modes. When there are multiple significant flexible modes, the application of input shaping on the additional modes also improves the performance.

7. REFERENCES

[1]. Junkins, J. L, Rahman, Z., and Bang, H., "Near-Minimum-Time Maneuvers of Flexible Vehicles: A Liapunov Control Law Design Method," *Mechanics and Control of Large Flexible Structures, Progress in Astronautics and Aeronautics,* Vol. 129, 1990, pp. 565-593.

[2]. Junkins, J. L, Rahman, Z., and Bang, H., "Near-Minimum-Time Control of Distributed Parameter Systems: Analytical and Experimental Results," *Journal of Guidance, Control, and Dynamics,* Vol. 14, No. 2, 1991, pp. 406-415.

[3]. Aspinwall, D. W., "Acceleration Profiles for Minimizing Residual Response," *Journal of Dynamic Systems, Measurement and Control*, Vol. 102, No. 1, 1980, pp. pp. 3-6.

[4]. Swigert, C. J., "Shaped Torque Techniques," *Journal of Guidance and Control*, Vol. 3, No. 5, 1980, pp. pp. 460-467.

[5]. Suk, J., Moon, J., and Kim, Y, "Torque Shaping Using Trigonometric Series Expansion for Slew of Flexible Structures," *Journal of Guidance, Control, and Dynamics*, vol. 21, No. 5, 1998, pp.698-703.

[6]. Hailey, J. A., "Experiment Verification of Attitude Control Techniques for Flexible Spacecraft Slew Maneuvers," Master Thesis, U.S. Naval Postgraduate School, March, 1992

[7]. Agrawal, B. N., and Hailey, L., "*Optimal Slew Maneuver of a Flexible Spacecraft-Analytical and Experimental Results*, IAF-92-0024, World Space Congress, Washington, D. C., August 28-September 5, 1992.

[8]. Agrawal, B. N., and Bang, H., "Robust Closed –Loop Control Design for Spacecraft Slew Maneuver Using Thrusters," *Journal of Guidance, Control, and Dynamics*, Vol. 18, No. 6, November-December 1995, pp 1336-1344.

[9]. Song, G., Buck, N. V., and Agrawal, B. N., "Spacecraft Vibration Reduction Using Pulse-width Pulse-Frequency Modulated Input Shaper," *Journal of Guidance, Control, and Dynamics*, Vol. 22, No. 3, pp. 433-440.

[10]. Singer, N. C., and Seering, W. P., "Preshaping Command Inputs to Reduce System Vibration," *Journal of Dynamic Systems, Measurement, and Control*, Vol. 112, March 1990, pp. 76-82.

[11]. Likins, P.W., and Fleischer, G. E., "*Results of Flexible Spacecraft Attitude Control Studies Utilizing Hybrid Coordinates,"* J. of Spacecraft and Rockets, Vol.8, March 1971, pp. 264-273.

Table 1 Natural Frequencies of the FSS

Mode	Cantilever (Hz)	System (Hz)
1	0.2510	0.2660
2	0.7084	0.7278
3	9.369	9.370
4	16.15	16.15
5	34.70	34.70
6	46.81	46.81
7	77.00	77.00
8	94.83	94.83

Table 2. Settling time comparison of the FSS maneuvered by four profiles

		No Input-Shaping		Shaping the first two modes using the ZVD method	
		bang-bang	versine (α=1)	bang-bang	versine (α=1)
T_{slew}(Simulation)		5.714	8.079	10.847	13.212
Without T_{ff}	t_{s1sim}	>> 30	~ 30	15.544	13.734
	t_{s2sim}	>> 30	>> 30	> 30	> 30
With T_{ff}	t_{s1sim}	> 30	22.33	10.848	13.213
	t_{s2sim}	> 30	> 30	28.283	16.652
T_{slew}(Experiments)		5.714	8.079	10.797	13.163
With T_{ff}	t_{s1exp}	29.873	20.973	10.797	13.163
	t_{s2exp}	>30	28.122	19.184	15.544

* (t_{s1sim}, t_{s2sim}) = settling time with $\Delta\theta_f = (0.015, 0.0015)\,\text{deg}$ respectively for simulations

* (t_{s1exp}, t_{s2exp}) = settling time with $\Delta\theta_f = (0.1, 0.05)\,\text{deg}$ respectively for experiments

Table 3. Comparison of the maximum residual vibration in simulations after 15 seconds

	No Input-Shaping		Shaping the first 2 modes with ZVD method	
	bang-bang	versine (α=1)	bang-bang	versine (α=1)
Without T_{ff}	(#1) 0.616 degree	(#2) 0.0664 degree	(#3) 0.0108 degree	(#4) 0.00787 degree
		To #1: 89.2%	To #1: 98.2%	To #1: 98.7%
				To #2: 88.1%
				To #3: 27.4%
With T_{ff}	(#5) 0.0674 degree	(#6) 0.0257 degree	(#7) 0.00416 degree	(#8) 0.00100 degree
	To #1: 89.1%	To #1: 95.8%	To #1: 99.3%	To #1: 99.8%
		To #2: 79.4%		To #2: 98.5%
		To #5: 61.8%		To #7: 76.0%
			To #3: 61.6%	To #4: 87.3%
			To #5: 93.8%	To #6: 96.1%

Note (1): The top and bottom halves of the table compare performance of input cases with or without torque feedforward (T_{ff}); the left and right halves of the table compare performance of input cases with or without input shaping of first 2 modes using the ZVD method.
Note (2): The sub-rows for each case give the information on which case the current case is compare to and how much % improvement it gets.

Table 4. Comparison of the maximum residual vibration in experiments after 20 seconds

	bang-bang	versine (α=1)
No input shaping	(#1) 0.174 degree	(#2) 0.113 degree
		To #1: 35.3%
Shaping 1 mode	(#3) 0.0301 degree	(#4) 0.0202 degree
	To #1: 82.7%	To #1: 88.4%
		To #2: 82.1%
		To #3: 32.9%
Shaping 2 modes	(#5) 0.0173 degree	(#6) 0.0205 degree
	To #1: 90.0%	To #1: 88.2%
		To #2: 81.8%

Note: The sub-rows for each case give the information of which case the current case is compare to and how much % improvement it gets. Torque feedforward is always applied in all experiments.

Figure 1. Flexible Spacecraft Simulator FSS)

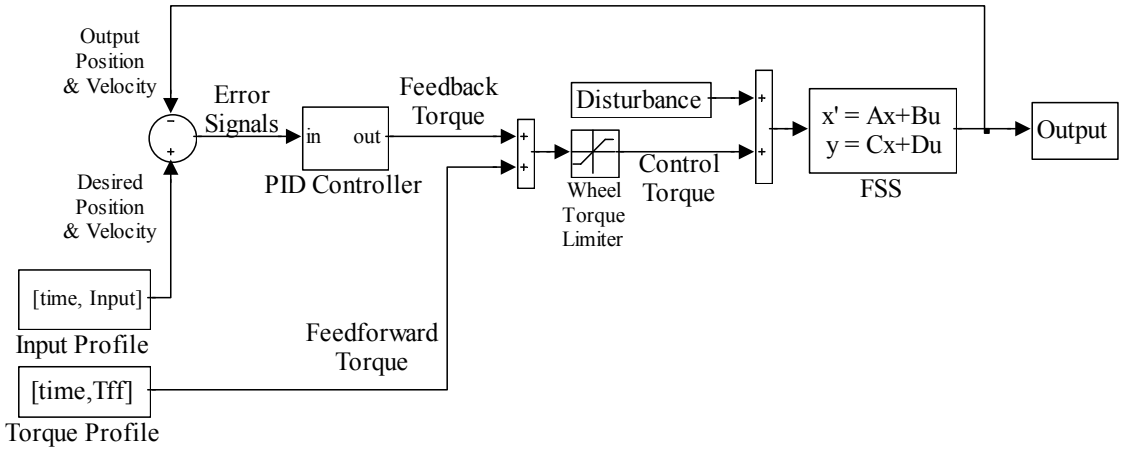

Figure 2 Slew Maneuver of NPS Flexible Spacecraft Simulator Using PID Control with Rate and Proportional Feedback

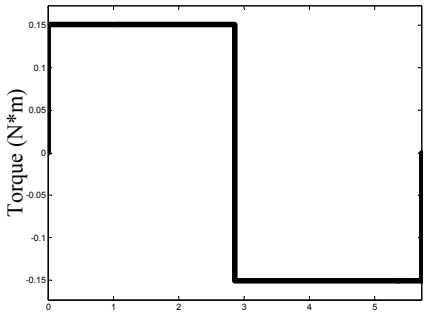

Figure 3. Bang-bang torque profiles without input shaping

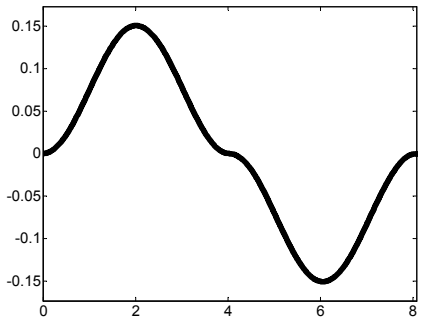

Figure 4. Versine Torque profiles without input shaping

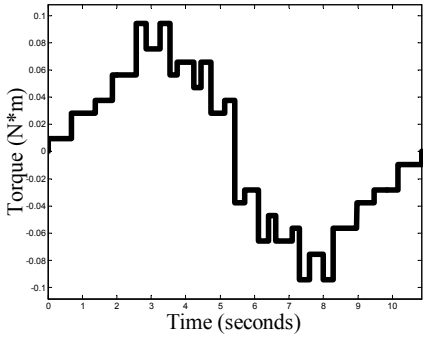

Figure 5. Bang-bang Torque profiles with input shaping (ZVD 2modes)

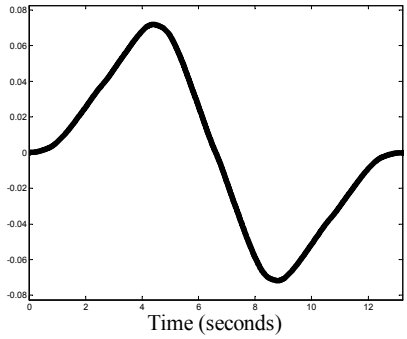

Figure 6. Versine Torque profiles with input shaping (ZVD 2 modes)

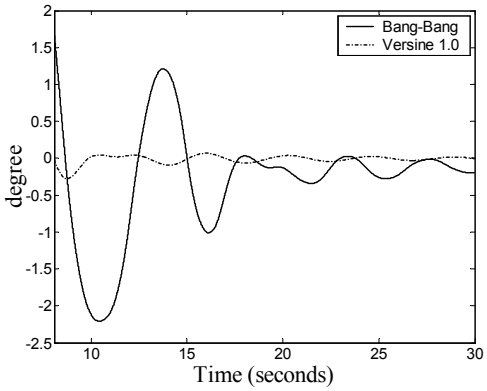

Figure 7. Residual vibration corresponding to using PID control (with rate feedback), without torque feedforward or input shaping, in simulation

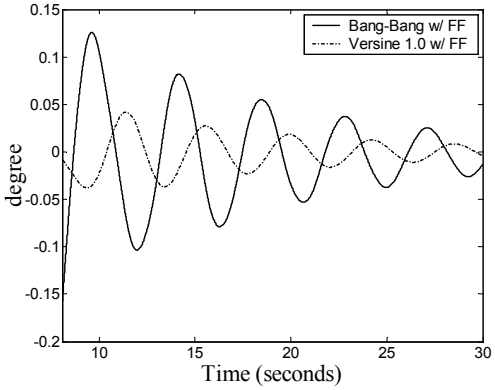

Figure 8. Same as Figure 7, except torque feedforward is now applied

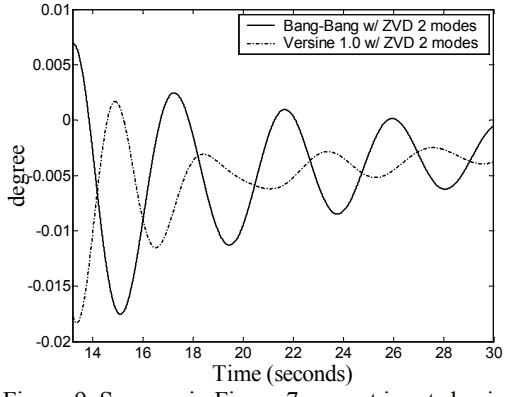

Figure 9. Same as in Figure 7, except input shaping of the first 2 modes with ZVD method is now applied

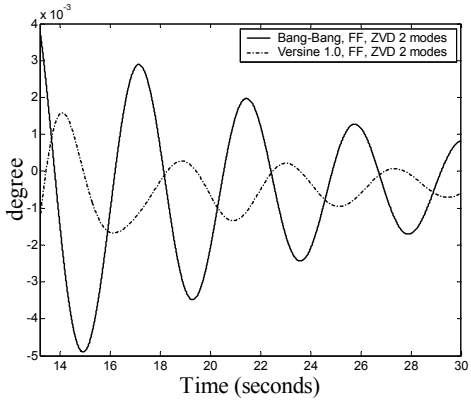

Figure 10. Same as Figure 7, with torque feedforward and input shaping of the first 2 modes using the ZVD method are now both applied

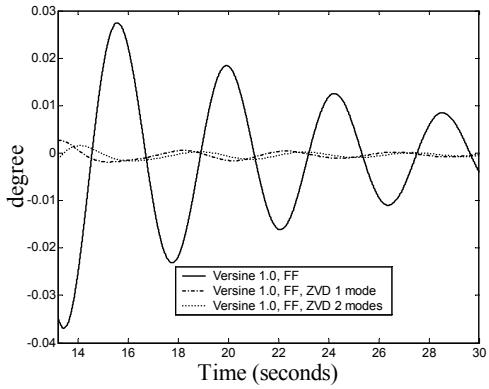

Figure 11. Residual vibration from using versine profiles with input shaping of 0, 1, or 2 modes (using ZVD method). (PID control with rate feedback, and torque feedforward applied in all three cases)

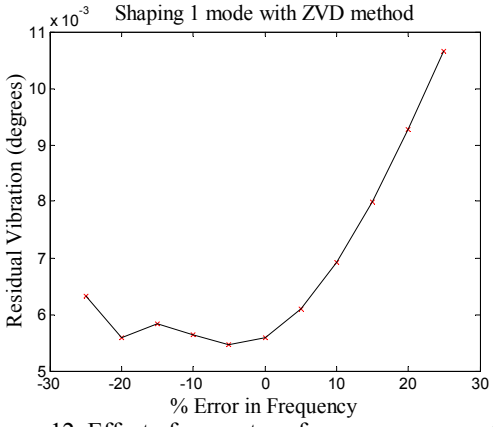

Figure 12. Effect of percentage frequency error on the maximum residual vibration, applying PI control (using rate feedback) with torque feedforward and input shaping 1 mode with ZVD method

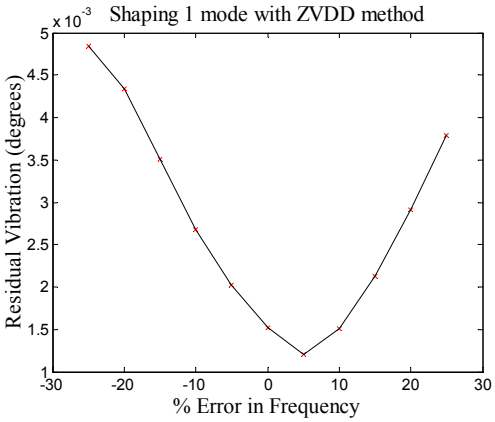

Figure 13. Effect of percentage frequency error on the maximum residual vibration, applying PI control (using rate feedback) with torque feedforward and input shaping 1 mode with ZVDD method

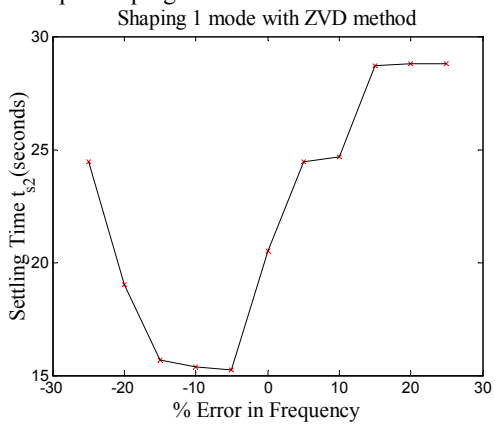

Figure 14. Effect of percentage frequency error on the settling time, applying PI control (using rate feedback) with torque feedforward and input shaping 1 mode with ZVD method

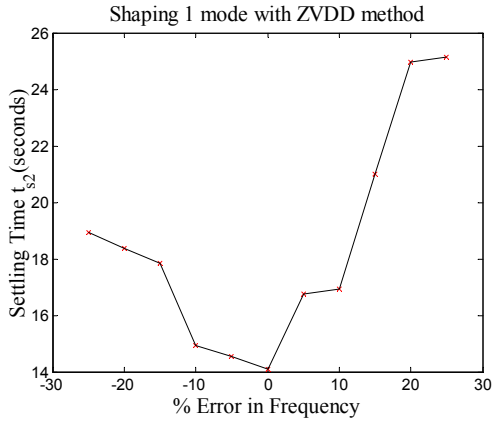

Figure 15. Effect of percentage frequency error on the settling time, applying PI control (using rate feedback) with torque feedforward and input shaping 1 mode with ZVDD method

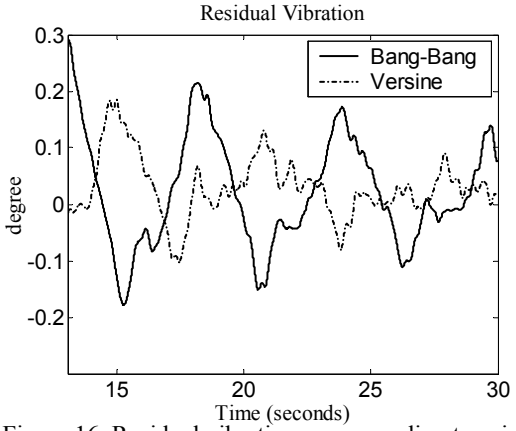

Figure 16. Residual vibration corresponding to using PID control (using rate feedback) with torque feedforward, but no input shaping, in experiments

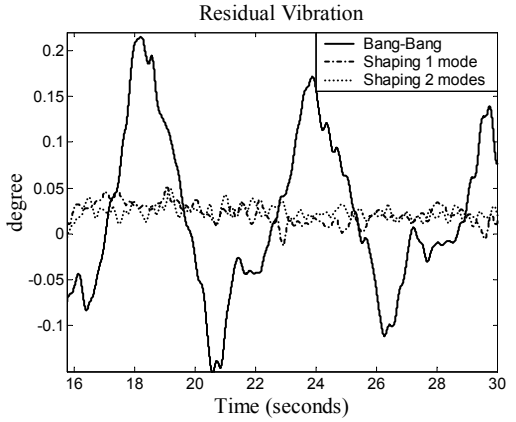

Figure 17. Residual Vibration corresponding to using PID control (using rate feedback) with torque feedforward and input shaping on bang-bang profile with ZVD method, in experiments

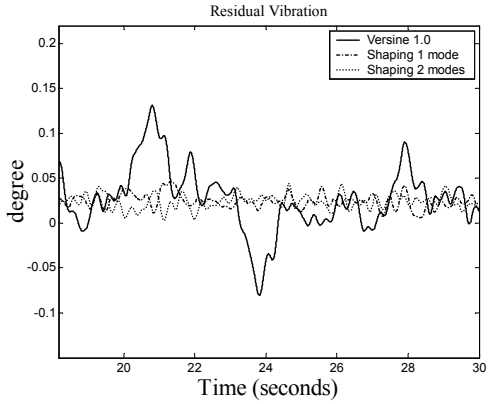

Figure 18. Residual Vibration corresponding to using PID control (using rate feedback) with torque feedforward and input shaping on versine profile (α=1) with ZVD method, in experiments

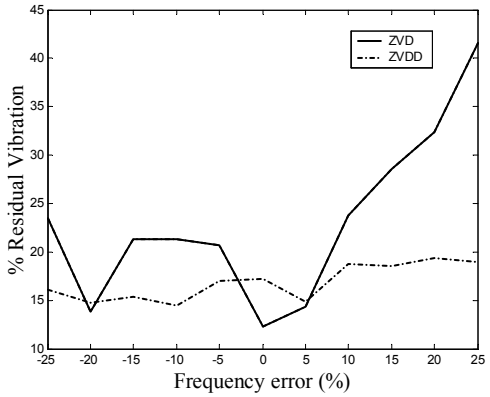

Figure 19. Effect of percentage frequency error on the percentage residual vibration, applying PID control (using rate feedback) with torque feedforward and input shaping first 2 mode with ZVD or ZVDD method